

Growth and optical properties of $\text{In}_x\text{Al}_y\text{Ga}_{1-x-y}\text{N}$ quaternary alloys

J. Li, K. B. Nam, K. H. Kim, J. Y. Lin, and H. X. Jiang

Citation: *Applied Physics Letters* **78**, 61 (2001); doi: 10.1063/1.1331087

View online: <http://dx.doi.org/10.1063/1.1331087>

View Table of Contents: <http://scitation.aip.org/content/aip/journal/apl/78/1?ver=pdfcov>

Published by the [AIP Publishing](#)

Articles you may be interested in

[Recombination dynamics of localized excitons in \$\text{Al}_x\text{In}_x\text{N}\$ epitaxial films on GaN templates grown by metalorganic vapor phase epitaxy](#)

J. Appl. Phys. **94**, 2449 (2003); 10.1063/1.1592868

[Luminescence mechanisms in quaternary \$\text{Al}_x\text{In}_y\text{Ga}_{1-x-y}\text{N}\$ materials](#)

Appl. Phys. Lett. **80**, 3730 (2002); 10.1063/1.1481766

[Time-resolved and time-integrated photoluminescence in ZnO epilayers grown on \$\text{Al}_2\text{O}_3\$ \(0001\) by metalorganic vapor phase epitaxy](#)

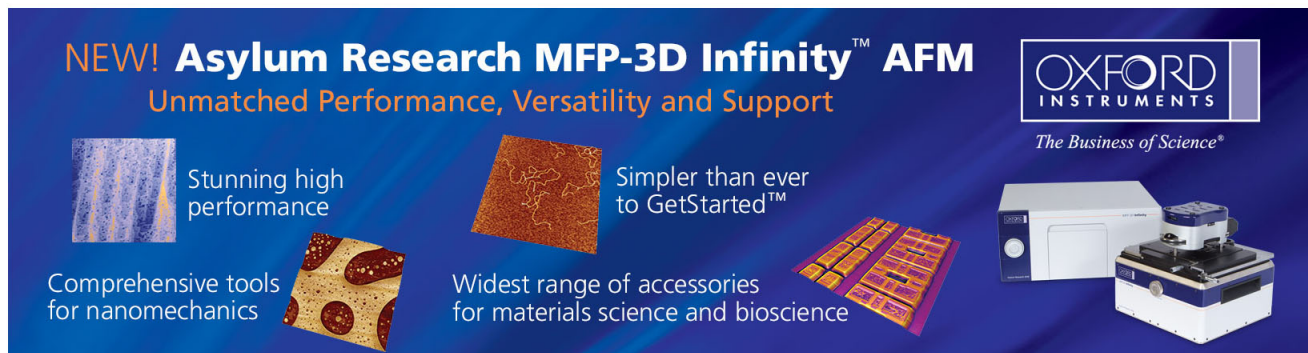
Appl. Phys. Lett. **80**, 1924 (2002); 10.1063/1.1461051

[Band gap bowing and exciton localization in strained cubic \$\text{In}_x\text{Ga}_{1-x}\text{N}\$ films grown on 3C-SiC\(001\) by rf molecular-beam epitaxy](#)

Appl. Phys. Lett. **79**, 3600 (2001); 10.1063/1.1421082

[Microphotoluminescence characterization of cleaved edge overgrowth T-shaped \$\text{In}_x\text{Ga}_{1-x}\text{As}\$ quantum wires](#)

J. Appl. Phys. **83**, 3777 (1998); 10.1063/1.367148

The advertisement features a dark blue background with white and orange text. At the top left, it reads 'NEW! Asylum Research MFP-3D Infinity™ AFM' in large white letters, followed by 'Unmatched Performance, Versatility and Support' in orange. To the right is the Oxford Instruments logo, which includes the text 'OXFORD INSTRUMENTS' and the tagline 'The Business of Science®'. Below the main text are four images: a blue textured surface, a brown textured surface, a yellow and red patterned surface, and a photograph of the MFP-3D Infinity AFM instrument. Each image is accompanied by a short text description: 'Stunning high performance', 'Simpler than ever to GetStarted™', 'Comprehensive tools for nanomechanics', and 'Widest range of accessories for materials science and bioscience'.

Growth and optical properties of $\text{In}_x\text{Al}_y\text{Ga}_{1-x-y}\text{N}$ quaternary alloys

J. Li, K. B. Nam, K. H. Kim, J. Y. Lin, and H. X. Jiang^{a)}

Department of Physics, Kansas State University, Manhattan, Kansas 66506-2601

(Received 16 August 2000; accepted for publication 9 October 2000)

$\text{In}_x\text{Al}_y\text{Ga}_{1-x-y}\text{N}$ quaternary alloys with different In and Al compositions were grown by metalorganic chemical vapor deposition. Optical properties of these quaternary alloys were studied by picosecond time-resolved photoluminescence. It was observed that the dominant optical transition at low temperatures in $\text{In}_x\text{Al}_y\text{Ga}_{1-x-y}\text{N}$ quaternary alloys was due to localized exciton recombination, while the localization effects in $\text{In}_x\text{Al}_y\text{Ga}_{1-x-y}\text{N}$ quaternary alloys were combined from those of InGaN and AlGaN ternary alloys with comparable In and Al compositions. Our studies have revealed that $\text{In}_x\text{Al}_y\text{Ga}_{1-x-y}\text{N}$ quaternary alloys with lattice matched with GaN epilayers ($y \approx 4.8x$) have the highest optical quality. More importantly, we can achieve not only higher emission energies but also higher emission intensity (or quantum efficiency) in $\text{In}_x\text{Al}_y\text{Ga}_{1-x-y}\text{N}$ quaternary alloys than that of GaN. The quantum efficiency of $\text{In}_x\text{Al}_y\text{Ga}_{1-x-y}\text{N}$ quaternary alloys was also enhanced significantly over AlGaN alloys with a comparable Al content. These results strongly suggested that $\text{In}_x\text{Al}_y\text{Ga}_{1-x-y}\text{N}$ quaternary alloys open an avenue for the fabrication of many optoelectronic devices such as high efficient light emitters and detectors, particularly in the ultraviolet region.

© 2001 American Institute of Physics. [DOI: 10.1063/1.1331087]

III nitrides including GaN epilayers, InGaN and AlGaN alloys, and InGaN/GaN and GaN/AlGaN multiple quantum wells (MQWs) have been intensively studied due to their many applications in ultraviolet (UV)/blue light emitters, solar-blind UV detectors, and high power/temperature electronics.¹ It has been demonstrated that most nitride based devices must take advantage of MQWs and heterostructures such as GaN/AlGaN and InGaN/GaN as well as the tunability of the band gaps in the alloys from InN (1.9 eV) to GaN (3.4 eV) and to AlN (6.2 eV). Thus an important issue is still quantum well (QW) or heterostructure device structural perfection, which requires development of innovative approaches to synthesize high quality III-nitride QWs and heterostructures. Recently, $\text{In}_x\text{Al}_y\text{Ga}_{1-x-y}\text{N}$ quaternary alloys have been recognized to have the potential to overcome some shortfall of GaN epilayers and InGaN and AlGaN alloys.²⁻⁷ By varying In and Al compositions x and y in $\text{In}_x\text{Al}_y\text{Ga}_{1-x-y}\text{N}$, one can change the energy band gap while keep lattice matched with GaN. In addition to the key features of lattice match with GaN and the tunability in energy band gap, $\text{In}_x\text{Al}_y\text{Ga}_{1-x-y}\text{N}$ quaternary alloys also have the potential to provide a better thermal match to GaN, which could be an important advantage in epitaxial growth. The potential applications of InAlGaN quaternary alloys as InGaN/InAlGaN QW light emitters,⁵ GaN/InAlGaN heterojunction field-effect transistors,⁷ and UV detectors⁸ have been demonstrated recently.

It was observed previously that photoluminescence (PL) emission intensity or quantum efficiency (QE) of $\text{Al}_x\text{Ga}_{1-x}\text{N}$ alloys decreases exponentially with an increase of Al content.⁹ QE of UV light emitters fabricated from $\text{Al}_x\text{Ga}_{1-x}\text{N}$ alloys are thus expected to drop significantly as the emission energy extends into deeper UV region. This is one of the key problems for the fabrication of high performance UV optoelectronic devices. In fact, in a recent proof-of-concept demonstration work, an output power of 13 μW

at 20 mA was measured from an AlGaN/GaN MQW light emitting diode (LED) in the UV spectral region near 354 nm.¹⁰ This output power is more than two orders of magnitude lower than a 3 mW output power from blue LEDs fabricated from InGaN/GaN MQWs.

In this letter, we report the growth and optical properties of $\text{In}_x\text{Al}_y\text{Ga}_{1-x-y}\text{N}$ quaternary alloys. A 0.5–1.0 μm GaN epilayer was first deposited on the sapphire substrate with a 25 nm low temperature GaN buffer layer, followed by the deposition of a 0.1 μm $\text{In}_x\text{Al}_y\text{Ga}_{1-x-y}\text{N}$ quaternary alloy epilayer by the low pressure metalorganic chemical vapor deposition (MOCVD). The growth temperature and pressure for the underneath GaN epilayer were 1050 °C and 300 Torr, respectively. For $\text{In}_x\text{Al}_y\text{Ga}_{1-x-y}\text{N}$ quaternary alloys, the growth temperature was 780 °C and In and Al compositions were controlled by varying the flow rates of TMI and TMAI. Picosecond time-resolved PL was employed to study the optical properties of these materials.¹¹ Contents of In and Al were determined by different methods including x-ray diffraction (XRD), energy dispersive system, Rutherford backscattering, and PL measurements and were within 5% variation. It was found that $\text{In}_x\text{Al}_y\text{Ga}_{1-x-y}\text{N}$ quaternary alloys with lattice matched with GaN epilayers ($y \approx 4.8x$) have the highest PL intensity as well as the narrowest XRD linewidth. Table I lists the optimal growth parameters and emission properties of one of the $\text{In}_x\text{Al}_y\text{Ga}_{1-x-y}\text{N}$ quaternary alloys that are lattice matched with GaN together with those of $\text{In}_x\text{Ga}_{1-x}\text{N}$ and $\text{Al}_x\text{Ga}_{1-x}\text{N}$ alloys. Room temperature electron mobilities and concentrations have also been measured and listed in Table I as well.

Figure 1 shows the PL emission spectra of GaN epilayer (No. 567), $\text{Al}_x\text{Ga}_{1-x}\text{N}$ alloy (No. 347), $\text{In}_x\text{Ga}_{1-x}\text{N}$ alloy (No. 693), and $\text{In}_x\text{Al}_y\text{Ga}_{1-x-y}\text{N}$ quaternary alloy (No. 706) measured at $T=10$ K. The arrows indicate the spectral peak positions. The integrated PL intensity, I_{emi} , for each of the alloy samples is included in Table I. The lower emission peak at 3.487 eV in the PL spectrum of InAlGaN quaternary alloy in Fig. 1(d) is due to the underneath GaN epilayer. The

^{a)}Electronic mail: Jiang@phys.ksu.edu

TABLE I. List of optimal growth parameters and PL emission properties of an $\text{In}_x\text{Al}_y\text{Ga}_{1-x-y}\text{N}$ quaternary alloy together with those of $\text{In}_x\text{Ga}_{1-x}\text{N}$ and $\text{Al}_x\text{Ga}_{1-x}\text{N}$ alloys.

		$\text{In}_x\text{Ga}_{1-x}\text{N}$	$\text{Al}_x\text{Ga}_{1-x}\text{N}$	$\text{In}_x\text{Al}_y\text{Ga}_{1-x-y}\text{N}$
Sample		KSU 693	KSU 347	KSU 706
Growth parameters	P (Torr)	300	270	300
	T ($^\circ\text{C}$)	780	1060	780
XRD (002) (arc sec)		359	375	411
In and Al contents		$x \sim 2.6\%$	$x \sim 13.6\%$	$x \sim 2.6\%$, $y \sim 12.4\%$
μ ($\text{cm}^2/\text{V s}$)		222	215	236
n (10^{17} cm^{-3})		2.50	5.40	3.60
E_p (eV)	$T=10 \text{ K}$	3.395	3.722	3.575
	$T=300 \text{ K}$	3.348	3.674	3.542
I_{emi} (a.u.)	$T=10 \text{ K}$	185	80	175
	$T=300 \text{ K}$	3.9	0.72	2.58
FWHM (meV)	$T=10 \text{ K}$	26	26	29
$E_{\text{activation}}$ (meV)		16.3	16.7	23.4
τ (ns) ($T=10 \text{ K}$)		0.28	0.35	0.49

emission spectrum of $\text{In}_x\text{Al}_y\text{Ga}_{1-x-y}\text{N}$ quaternary alloys in Fig. 1(d) shows that we can achieve not only higher emission energies but also higher emission efficiency in $\text{In}_x\text{Al}_y\text{Ga}_{1-x-y}\text{N}$ quaternary alloys than that of GaN. The physical origin of this enhanced QE in $\text{In}_x\text{Al}_y\text{Ga}_{1-x-y}\text{N}$ quaternary alloys over GaN and $\text{Al}_x\text{Ga}_{1-x}\text{N}$ alloy is not yet clear. However, it is now well known that $\text{In}_x\text{Ga}_{1-x}\text{N}$ alloys have higher QE than GaN epilayers. It is thus not surprising that the QE is enhanced after the incorporation of indium into $\text{Al}_x\text{Ga}_{1-x}\text{N}$.

PL spectra at different temperatures were also measured for InAlGaN, InGaN, and AlGaN alloys. Emission intensities in these samples all decrease with increasing tempera-

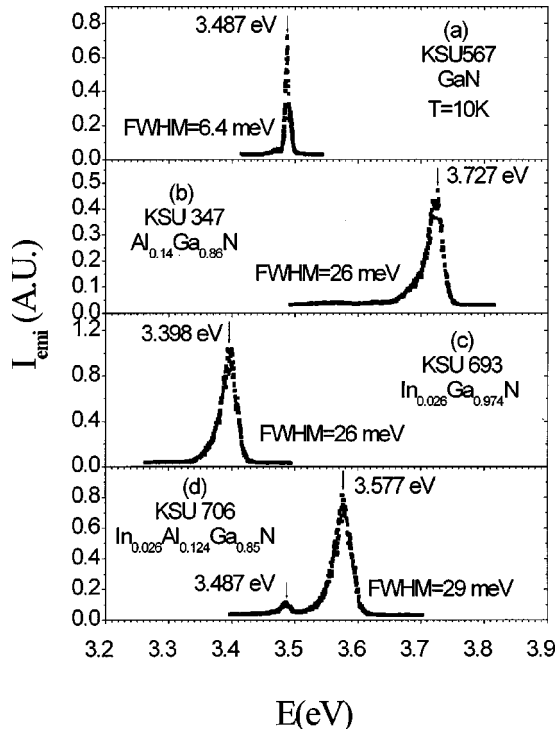


FIG. 1. PL spectra of GaN, $\text{Al}_x\text{Ga}_{1-x}\text{N}$, $\text{In}_x\text{Ga}_{1-x}\text{N}$, and $\text{In}_x\text{Al}_y\text{Ga}_{1-x-y}\text{N}$ quaternary alloys measured at $T=10 \text{ K}$. The emission spectrum of $\text{In}_x\text{Al}_y\text{Ga}_{1-x-y}\text{N}$ shows that we can achieve not only higher emission energies but also higher emission efficiency in InAlGaN quaternary alloys than that of GaN. The emission efficiency of $\text{In}_x\text{Al}_y\text{Ga}_{1-x-y}\text{N}$ is also higher than that of $\text{Al}_x\text{Ga}_{1-x}\text{N}$ and is comparable to that of $\text{In}_x\text{Ga}_{1-x}\text{N}$.

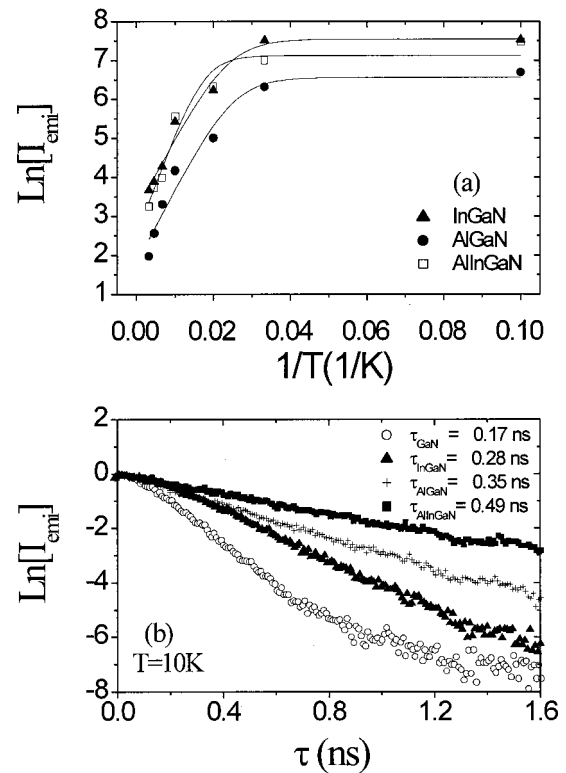


FIG. 2. (a) The Arrhenius plots of PL intensities of InAlGaN, InGaN, and AlGaN alloys. (b) PL decay profile of InAlGaN together with those of GaN epilayers, InGaN, and AlGaN alloys measured at $T=10 \text{ K}$.

ture. The Arrhenius plots of PL intensity of InAlGaN, InGaN, and AlGaN alloys are shown in Fig. 2(a). The solid lines in Fig. 2(a) are the least squares fit of data with the equation

$$I(T) = I_0 / [1 + C \exp(-E_0/kT)], \quad (1)$$

where E_0 is the activation energy and C is a fitting constant. The fitted values of E_0 are 16.3, 16.7, and 23.4 meV for InGaN, AlGaN, and InAlGaN alloys, respectively.

From Table I, it is interesting to note that the growth conditions as well as the emission properties of $\text{In}_x\text{Al}_y\text{Ga}_{1-x-y}\text{N}$ are more closely related with $\text{In}_x\text{Ga}_{1-x}\text{N}$ than $\text{Al}_x\text{Ga}_{1-x}\text{N}$. The growth temperature and pressure for the optimized $\text{In}_x\text{Al}_y\text{Ga}_{1-x-y}\text{N}$ quaternary alloys ($T_g=780 \text{ }^\circ\text{C}$ and $P=300 \text{ } \tau$) are exactly the same as for $\text{In}_x\text{Ga}_{1-x}\text{N}$ alloys. The relative integrated PL intensities of $\text{In}_x\text{Al}_y\text{Ga}_{1-x-y}\text{N}$ quaternary alloys are 175 ($T=10 \text{ K}$) and 2.58 ($T=300 \text{ K}$). These values are comparable with the values of 185 ($T=10 \text{ K}$) and 3.9 ($T=300 \text{ K}$) for InGaN, but much larger than the values of 80 ($T=10 \text{ K}$) and 0.72 ($T=300 \text{ K}$) for AlGaN. It is thus concluded that $\text{In}_x\text{Al}_y\text{Ga}_{1-x-y}\text{N}$ quaternary alloys are InGaN-like rather than AlGaN-like, although Al composition is almost a factor of 5 larger than In.

The dominant PL transitions in $\text{In}_x\text{Al}_y\text{Ga}_{1-x-y}\text{N}$ quaternary alloys at low temperatures are also due to the localized exciton recombination, just as the cases in InGaN and AlGaN alloys. This fact is reflected in the characteristics of time-resolved PL as well as decay lifetimes. Decay lifetimes of PL emission at their spectral peak positions were also measured for InAlGaN, InGaN, and AlGaN alloys and Fig. 2(b) shows the PL decay profiles measured at their corre-

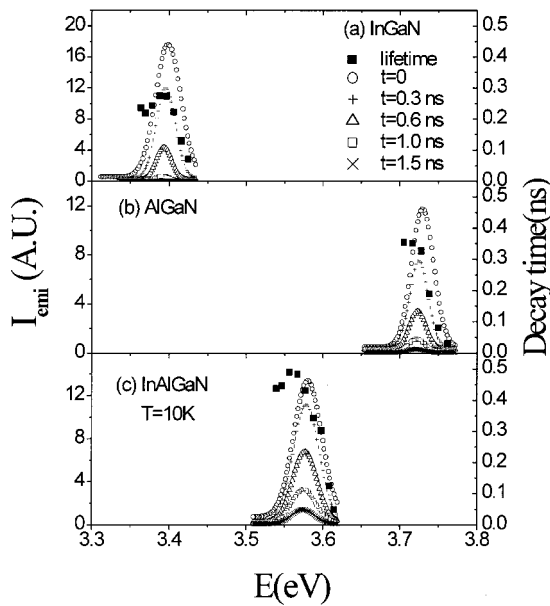


FIG. 3. Time-resolved PL spectra as well as emission energy dependence of decay lifetime measured at 10 K for (a) $\text{In}_x\text{Ga}_{1-x}\text{N}$ alloys, (b) $\text{Al}_x\text{Ga}_{1-x}\text{N}$ alloys, and (c) $\text{In}_x\text{Al}_y\text{Ga}_{1-x-y}\text{N}$ quaternary alloys.

sponding spectral peak positions at 10 K. The measured decay lifetimes at 10 K for InGaN, AlGaIn, and InAlGaIn alloys are listed in Table I.

In Fig. 3 is the plot of time-resolved PL spectra as well as emission energy dependence of decay lifetime measured at $T=10$ K for (a) $\text{In}_x\text{Ga}_{1-x}\text{N}$, (b) $\text{Al}_x\text{Ga}_{1-x}\text{N}$, and (c) $\text{In}_x\text{Al}_y\text{Ga}_{1-x-y}\text{N}$. The behavior of emission energy dependence of decay lifetime is very similar among these three alloys. While InAlGaIn has the longest decay lifetimes, the decay lifetime decreases with an increase of emission energy at energies above their corresponding spectral peak positions. This is a well-known character of localized excitons and is due to the transfer of excitons from higher to lower energy sites within the tail states caused by alloy fluctuations.¹²

The increased decay lifetime as well as activation energy in quaternary alloys points to an enhanced localization effects in $\text{In}_x\text{Al}_y\text{Ga}_{1-x-y}\text{N}$ quaternary alloys compared with InGaN and AlGaIn ternary alloys. The measured PL decay lifetime for $\text{In}_x\text{Al}_y\text{Ga}_{1-x-y}\text{N}$ quaternary alloys at $T=10$ K, from Table I, is 0.49 ns, while that for InGaN and AlGaIn are 0.28 and 0.35 ns, respectively. It is interesting that the measured decay lifetime of $\text{In}_x\text{Al}_y\text{Ga}_{1-x-y}\text{N}$ quaternary alloys at $T=10$ K, τ_{InAlGaIn} , is correlated with those of InGaN and AlGaIn alloys, τ_{InGaIn} and τ_{AlGaIn} , through with the relation $\tau_{\text{InAlGaIn}} = 0.49 \text{ ns} \approx (\tau_{\text{InGaIn}}^2 + \tau_{\text{AlGaIn}}^2)^{1/2} = (0.28^2 + 0.35^2)^{1/2} = 0.45 \text{ ns}$. This fact provides some hint that localization effects in $\text{In}_x\text{Al}_y\text{Ga}_{1-x-y}\text{N}$ quaternary alloys are the summation of those in AlGaIn and InGaIn alloys with comparable In and Al compositions. Further evidence to support this speculation is that the relation between the activation energies, E_0 , in $\text{In}_x\text{Al}_y\text{Ga}_{1-x-y}\text{N}$ and InGaIn and AlGaIn as shown in Table I is the same as the decay lifetimes, i.e., $E_{0,\text{InAlGaIn}} = 23.4 \text{ meV} \approx (E_{0,\text{AlGaIn}}^2 + E_{0,\text{InGaIn}}^2)^{1/2} = (16.3^2 + 16.7^2)^{1/2} \text{ meV} = 23.3 \text{ meV}$.

The important implication here is that not only $\text{In}_x\text{Al}_y\text{Ga}_{1-x-y}\text{N}$ quaternary alloys can provide lattice match with GaN, but also the emission intensity of

$\text{In}_x\text{Al}_y\text{Ga}_{1-x-y}\text{N}$ quaternary alloys is also much higher than that of AlGaIn with a comparable Al composition. The enhanced emission intensity or QE have been observed recently in unstrained InGaIn/InAlGaIn QWs and was attributed to the reduction of dislocation density as well as of the piezoelectric field.⁵ Our results show that besides the advantages of reducing dislocation density and/or piezoelectric field in lattice-matched InGaIn/InAlGaIn and GaIn/InAlGaIn QWs, emission intensity or QE of InAlGaIn is also higher than that of AlGaIn with a comparable Al composition. This makes the InAlGaIn quaternary alloys a better choice for many UV optoelectronic applications over AlGaIn. It is expected that detrimental effects due to lattice mismatch between the barrier and well materials, such as layer cracking, piezoelectric field, and high dislocation density will be significantly reduced in devices based on quaternary alloys compared with those utilizing ternary alloys. This is very important for UV emitter applications, where either AlGaIn or InAlGaIn will be used as active layers.

In summary, $\text{In}_x\text{Al}_y\text{Ga}_{1-x-y}\text{N}$ quaternary alloys have been grown by MOCVD on sapphire substrates. Optical properties of $\text{In}_x\text{Al}_y\text{Ga}_{1-x-y}\text{N}$ quaternary alloys have been studied by picosecond time-resolved PL spectroscopy and compared with those of GaN epilayers as well as InGaIn and AlGaIn alloys. By controlling In and Al compositions of $\text{In}_x\text{Al}_y\text{Ga}_{1-x-y}\text{N}$ quaternary alloys, we can achieve not only lattice match with GaN but also higher emission energies as well as higher emission efficiencies in the UV region in $\text{In}_x\text{Al}_y\text{Ga}_{1-x-y}\text{N}$ quaternary alloys than that in GaN epilayers. In addition, PL emission intensity or quantum efficiency of $\text{In}_x\text{Al}_y\text{Ga}_{1-x-y}\text{N}$ quaternary alloys is enhanced over $\text{Al}_x\text{Ga}_{1-x}\text{N}$ alloys with similar Al contents and is comparable to that of $\text{In}_x\text{Ga}_{1-x}\text{N}$ alloys with similar In composition. It is also demonstrated that the physical properties of $\text{In}_x\text{Al}_y\text{Ga}_{1-x-y}\text{N}$ quaternary alloys are more closely related with $\text{In}_x\text{Ga}_{1-x}\text{N}$ than $\text{Al}_x\text{Ga}_{1-x}\text{N}$ including growth conditions and material properties.

This research is supported by the grants from DOE (96ER45604), NSF (DMR-9902431 and INT-9729582), ARO, ONR, and BMDO.

¹S. Nakamura and G. Fasol, *The Blue Laser Diode* (Springer, New York, 1997).

²F. G. McIntosh, K. S. Boutros, J. C. Roberts, S. M. Bedair, E. L. Piner, and N. A. El-Masty, *Appl. Phys. Lett.* **68**, 40 (1996).

³M. E. Aumer, S. F. LeBoeuf, F. G. McIntosh, and S. M. Bedair, *Appl. Phys. Lett.* **75**, 3315 (1999).

⁴S. F. LeBoeuf, M. E. Aumer, and S. M. Bedair, *Appl. Phys. Lett.* **77**, 97 (2000).

⁵M. E. Aumer, S. F. LeBoeuf, S. M. Bedair, M. Smith, J. Y. Lin, and H. X. Jiang, *Appl. Phys. Lett.* **77**, 821 (2000).

⁶M. Asif Khan, J. W. Yang, G. Simin, R. Gaska, M. S. Shur, and A. D. Bykhovskii, *Appl. Phys. Lett.* **75**, 2806 (1999).

⁷M. Asif Khan, J. W. Yang, G. Simin, R. Gaska, M. S. Shur, H.-C. zur Loye, G. Tamulaitis, A. Zukauskas, D. J. Smith, D. Chandrasekhar, and R. Bicknell-Tassius, *Appl. Phys. Lett.* **76**, 1161 (2000).

⁸T. N. Oders, J. Li, J. Y. Lin, and H. X. Jiang, *Appl. Phys. Lett.* **77**, 791 (2000).

⁹H. S. Kim, R. A. Mair, J. Li, J. Y. Lin, and H. X. Jiang, *Appl. Phys. Lett.* **76**, 1252 (2000).

¹⁰J. Han, M. H. Crawford, R. J. Shul, J. J. Figiel, M. Bansa, L. Zhang, Y. K. Song, H. Zhou, and A. V. Nurmikko, *Appl. Phys. Lett.* **73**, 1688 (1998).

¹¹<http://www.phys.ksu.edu/area/GaNgroup/>

¹²R. A. Mair, J. Y. Lin, H. X. Jiang, E. D. Jones, A. A. Allerman, and S. R. Kurtz, *Appl. Phys. Lett.* **76**, 188 (2000).